

Evaluation of cyclic plasticity models of multi-surface and non-linear hardening by an energy-based fatigue criterion[†]

Shahram Shahrooi^{*}, Ibrahim Henk Metselaar and Zainul Huda

Center of Research for Advanced Materials, University of Malaya, Kuala Lumpur, Malaysia

(Manuscript Received June 8, 2009; Revised January 28, 2010; Accepted February 7, 2010)

Abstract

This study examines the performance of four constitutive models according to capacity in predicting metal fatigue life under proportional and non-proportional loading conditions. These cyclic plasticity models are the multi-surface models of Mroz and Garud, and the non-linear kinematic hardening models of Armstrong-Frederick and Chaboche. The range of abilities of these models is studied in detail. Furthermore, the plastic strain energy under multiaxial fatigue condition is calculated in the cyclic plasticity models by the stress-strain hysteresis loops. Using the results of these models, the fatigue lives that have set in the energy-based fatigue model are predicted and evaluated with the reported experimental data of 1% Cr-Mo-V steel in the literature. Consequently, the optimum model in the loading condition for this metal is chosen based on life factor.

Keywords: Multi-surface plasticity model; Non-linear plasticity model; Energy-based fatigue model; Multiaxial fatigue

1. Introduction

The study of multiaxial fatigue damage requires a thorough understanding of plasticity. Fatigue-crack initiation as controlled by local plasticity is a well-accepted phenomenon. Fatigue failure of mechanical components is a process comprising cyclic stress/strain evolutions and redistributions in the critical stressed volume. Due to stress concentration (notches, material defects, or surface roughness), the local material yields and redistributes the loading to the surrounding material, then follows it with cyclic plastic deformation. Finally, a crack is initiated leading to the loss of the resistance. Therefore, simulations for cyclic stress-strain evolution and redistribution are critical for predicting fatigue failure of mechanical components. Diverse criteria such as stress, strain, energy, and critical plane criterion have been utilized to estimate fatigue life of metals [1-6]. The earliest fatigue life prediction approach used the stress range as fatigue parameter for life correlations [7], and its models are suitable for high cycle fatigue. Soon after, the strain range was recognized as fatigue parameter for life prediction [8].

The parameters are typically associated with low cyclic fatigue. More recently, the energy parameter [9] that considers both stress range and strain range has been developed for life

predictions, in reaction to the differences between stress response and strain response in plastic deformations. In this paper, energy-based criteria of multiaxial fatigue are utilized. Morrow [10] and Halford [11] performed detailed investigations of the hysteresis loop shape and stable plastic work per cycle during fatigue. The proposed relation between plastic strain energy and fatigue life has been developed in terms of the fatigue properties. These properties are determined using the Coffin-Manson equation. This equation is the summation of two separate curves for elastic and plastic strain amplitude-life. When plotted on log-log scales, both curves become straight lines. Garud [12] suggested applying the uniaxial hysteresis loop energy concepts of Morrow to multiaxial fatigue. The model of Jahed and Varvani-Farahani [13] expresses the total energy consisting of two parts, plastic and elastic strain energies, where the plastic strain is related to the hysteresis loop loading shape.

A variety of plasticity models has been introduced to estimate the material cyclic deformation [14-17]. Prager [18] in 1956 was the first to introduce kinematic hardening. The plastic modulus calculation in the model is coupled with its kinematic hardening rule through the yield surface compatibility condition. The Armstrong-Frederick [19] and Chaboche [20-22] non-linear kinematic hardening models belong to this group. In other plasticity models, such as the Mroz [23, 24] and Garud [25] multi-surface models, the plastic modulus computation is not coupled to the kinematic hardening rule.

In this study, two multi-surface and two non-linear kinemat-

[†] This paper was recommended for publication in revised form by Associate Editor Chongdu Cho

^{*} Corresponding author. Tel.: +60 3 7967 4598, Fax.: +60 3 7967 5317

E-mail address: shahramshahrooie@yahoo.com

© KSME & Springer 2010

ic hardening models of cyclic plasticity for fatigue life prediction of metals are analyzed and simulated in proportional and non-proportional loadings. The life prediction is performed by a plastic strain energy model, and the plasticity models are examined using their life factors.

2. Cyclic plasticity

The correlation of cyclic plasticity with fatigue, fracture, and deformation cases of industrial pieces has been focused on by many researchers [26, 27].

The three basic assumptions of an incremental plasticity model are as follows:

1. Yield condition
2. Flow rule
3. Consistency condition

The yield surface for boundary recognition between elastic and elastic-plastic regions in the multiaxial loadings is utilized, where the stress point is always on the yield surface boundary. Based on flow or normality rule, the plastic increment is always normal to the yield surface. The consistency condition shows that by reversing the load direction during any plastic loading, the behavior of the metal is always elastic. During plastic loading, the yield surface boundary follows the stress in the stress space. The consistency condition is the root of the hardening rules. There are general viewpoints for yield surface based on the hardening rules. The most important use of kinematic hardening is determined when the inverse loading subjects are present. Isotropic hardening is able to handle any proportional and non-proportional loading. However, this hardening rule is unable to simulate the stress-strain hysteresis loop in cyclic loadings. Therefore, for simulation process, the kinematic hardening will be used in this study.

2.1 Stress-Strain relation in kinematic hardening in the multiaxial case

Based on the Prager rule for satisfying the consistency condition, yield stress moves without any expansion to follow the stress point in the stress space. In the Prager plasticity model, the movement of the yield surface is parallel to the plastic increment:

$$da_{ij} = cd\varepsilon_{ij}^p \quad (1)$$

In other words, the movement of the yield surface is in the direction of the instantaneous normal vector, as shown in Fig. 1.

The stress-strain relations for the kinematic hardening rule are formulated by combining the following:

Yield condition is

$$F = \frac{3}{2}(S_{ij} - a_{ij})(S_{ij} - a_{ij}) - \sigma_{y0} = 0 \quad (2)$$

b) The flow rule is $d\varepsilon_{ij}^p = \frac{dS_{kl}n_{kl}}{K_p}n_{ij}$ (3)

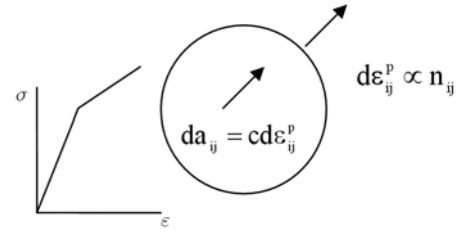


Fig. 1. Prager rule.

c) The hardening rule is $da_{ij} = cd\varepsilon_{ij}^p$

d) The consistency condition is

$$dS_{ij}(S_{ij} - a_{ij}) = da_{ij}(S_{ij} - a_{ij}) \quad (4)$$

The normal unit vector for kinematic hardening is defined

as $n_{ij} = \sqrt{\frac{3}{2}} \frac{(S_{ij} - a_{ij})}{\sigma_{y0}}$ (5)

Using Eq. (5), the flow rule, hardening rule, and stress-strain relation will be defined as

$$d\varepsilon_{ij}^p = \frac{3}{2} \frac{(S_{kl} - a_{kl})dS_{kl}}{c\sigma_{y0}^2} (S_{ij} - a_{ij}) \quad c = K_p \quad (6)$$

where S_{ij} and dS_{ij} are the stress tensor and its increment, respectively; a_{ij} and da_{ij} are the centers of the moveable yield surface or back stress and its increment; and K_p is the multiaxial representation of the plastic tangent modulus.

2.2 Multi-surface models

2.2.1 Mroz model

For better approximation of the stress-strain curve and generalization of the plastic modulus in multiaxial case, Mroz [24] defined a field of different plastic modulus in the stress space.

During plastic loading, these stress surfaces are activated subsequently and move until the stress point meets the next stress inactive stress surface. When the stress point meets a stress surface, this surface is active. By increasing the load, the active surface and the entire, previously activated surface (inner surfaces) move together until unloading occurs. To find the direction of the movement for active stress surfaces, the steps in the non-proportional loading are as follows:

1. Find a similar point on the next surface that has the same normal vector as the current normal vector:

$$S_{ij}^* = \frac{R_{k+1}}{R_k} (S_{ij} - a_{ij}) + a_{ij}^{k+1} \quad (7)$$

2. Determine the direction of the center of active surface:

$$da_{ij}^k = d\eta(S_{ij}^* - S_{ij}) \quad (8)$$

3. Other inner surfaces $1 < k < k-1$ need to be in touch with the active surface during plastic loading.

In this situation, the back stress of the other internal surfaces is as follows:

$$a_{ij}^r = S_{ij} - \sqrt{\frac{2}{3}} R_r n_{ij}, 1 < r < k-1 \quad (9)$$

where S_{ij}^* is a point of the next stress surface that has the same normal vector as the present stress surface. The scalar value of $d\alpha$ is computable from the consistency relation.

2.2.2 Garud model

Movement of the surface in the Garud model is dependent on the stress direction. The following steps are needed to determine the movement direction of the yield surface based on the Garud model:

1. Find the normal vector on the next surface:

$$n_{ij}^B = \sqrt{\frac{3}{2}} \frac{S_{ij}^B - a_{ij}^{k+1}}{R_{k+1}} \quad (10)$$

2. Find the stress point on the next inactive surface S_{ij}^B by extending the current stress increment. Here, S_{ij}^* is a similar point on the active surface. These have the same normal vectors as

$$S_{ij}^* = \sqrt{\frac{2}{3}} R_k n_{ij}^* + a_{ij}^k \quad (11)$$

3. Determine the direction of the center of active surface: $da_{ij}^k = d\eta(S_{ij}^B - S_{ij}^*)$ (12)

Other inner surfaces such as $1 < k < k-1$ will be in touch with the active surface during plastic loading, similar to the situation of the Mroz model.

2.3 Non-linear kinematic hardening model

2.3.1 Armstrong–Frederick model

Armstrong and Frederick [19] added non-linear parameter to the Prager model for better estimation of the stress-strain curve in uniaxial and multiaxial loadings. The kinematic hardening rule for the yield surface utilized in this model has been added to the first term by

$$da_{ij} = cd\varepsilon_{ij}^p - \gamma a_{ij} d\varepsilon_e^p \quad (13)$$

where, c and γ are material constants obtained from cyclic stress-strain curve, and $d\varepsilon_e^p$ is the equivalent plastic increment. One of the evident properties of this model is coupled to the plastic modulus of the hardening functions. The equation in the uniaxial loading condition is transformed into a relation between moving yield surface and plastic strain. The equation yields an increasing curve; however, the gradient of this curve is decreased by the increasing stress and the equation value tends to become the constants c/γ . The plastic modulus in the hardening rule is found by multiplying n_{ij} in Eq. (13) with the following flow rule and consistency condition:

$$K_p = c - \gamma a_{ij} n_{ij}. \quad (14)$$

2.3.2 Chaboche model

Instead of one term, Chaboche [20] used several terms similarly used in the initial model of Armstrong-Frederick for determining the yield surface center variations.

$$da_{ij} = \sum_{k=1}^M da_{ij}^k \quad da_{ij}^k = \frac{2}{3} c_k d\varepsilon_{ij}^p - \gamma_k a_{ij}^k d\varepsilon_e^p, 1 \leq k \leq m \quad (15)$$

Although the Chaboche model was presented with three terms ($m=3$) the number of these terms has been increased.

3. Procedure of fatigue life prediction

A computer program is developed to simulate stress-strain response numerically in order to calculate strain energy based on the back stress values in the plasticity model. The elastic-plastic stiffness tensor is used in the computer program for incremental loading. Using increments of strain, the stress increments and plastic strains are calculated for different values of strain increment. The plastic work per cycle under non-proportional loading is calculated by integrating both axial and torsional hysteresis loops. The values of fatigue life in different loading conditions are predicted using the plastic part of the energy-based proposed method of Jahed and Varvani-Farahani [13]:

$$\begin{cases} \Delta W_A^p = E_f' (N_A)^C \\ \Delta W_T^p = W_f' (N_T)^{C_2} \end{cases} \quad (16)$$

N_A and N_T are calculated by utilizing the fatigue coefficient obtained from the energy-fatigue life curve. Plastic strain energy values are determined from the last step. The fatigue lives in the plasticity models are calculated with the help of the following equation from the energy method:

$$N_f = \frac{\Delta W_A}{\Delta W} N_A + \frac{\Delta W_T}{\Delta W} N_T. \quad (17)$$

4. Evaluation of the plasticity models

In this study, the results of the fatigue life prediction of the plasticity models of Mroz and Garud (multi-surface models) and Armstrong-Frederick and Chaboche (non-linear models) are compared with the experimental results of Brown and Miler [28, 29] on 1% Cr-Mo-V steel. The data include proportional and non-proportional tension-torsion tests with several loading paths and strain ratios. The energy-based fatigue coefficients are shown in Table I.

4.1 Mroz model

Predicted fatigue lives obtained by this model are plotted

Table 1. Energy-based fatigue coefficients.

Value		Value	
Axial		Torsional	
$E_f'(MJ/m^3)$	1139.32	$W_f'(MJ/m^3)$	2674.78
C	-0.765	C_s	-0.7816

Table 2. Chaboche constants for each back stress.

Number of l 2 back stress	1	2	3	4
Constant c	11235.5	13267.2	13961.8	1622.5
Constant γ	425.9	250.1	250.1	0

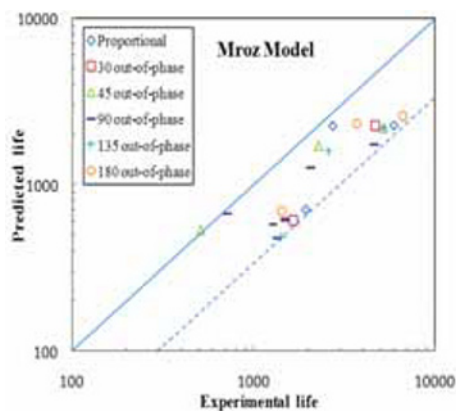


Fig. 2. Life prediction using the Mroz plasticity model.

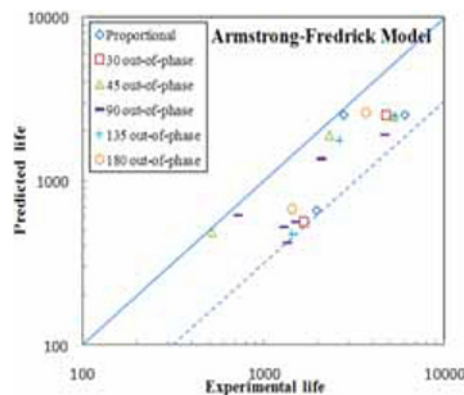


Fig. 4. Life prediction using the Armstrong-Fredrick plasticity model.

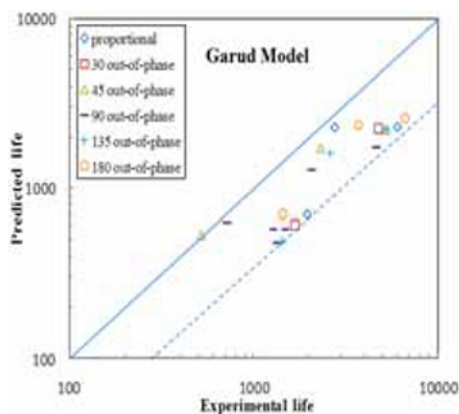


Fig. 3. Life prediction using the Garud plasticity model.

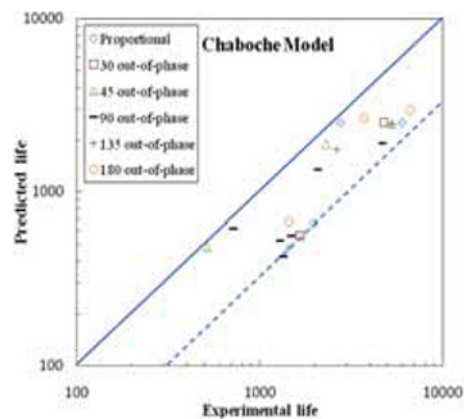


Fig. 5. Life prediction using the Chaboche plasticity model.

versus the experimental life in Fig. 2. Some results are close to a factor of 3. The correlation of fatigue life values of predicted and experimental lives is satisfactory for proportional and non-proportional loadings.

4.2 Garud model

Fig. 3 shows that the prediction of this plasticity model is very close to the value of the Mroz model. The effect on the results is observably distinct. Nevertheless, the results of the Garud model are numerically closer to the experimental results than to any other model.

4.3 Armstrong-frederick model

From the cyclic stress-strain curve of material constants, c, γ are determined to be 33322.2 and 194.5, respectively. The predicted life obtained by using the present parameter is compared to the experimental life data in Fig. 4 and the maximum life factor of 3.1.

4.4 Chaboche model

In this model, the number of back stress from approximation stress strain curve is 4. Material constants c, γ are listed in Table II. These constants are determined by using the least square method.

The predicted fatigue lives under proportional and non-proportional loading conditions obtained by the simulation method are compared to the experimental life data in Fig. 5. The maximum fatigue life correlation factor is equal to 3.1.

5. Discussion

Figs. 2-5 show that the fatigue life predicted used in the model fatigue of the plastic strain energy produced results approximately similar to those of the plasticity models of the multi-surface and non-linear under proportional and non-proportional loadings. For similar loading conditions, on this metal of maximum life factors in the multi-surfaces plasticity

Table 3. Maximum life factors on the energy model.

Plasticity models		Mroz	Garud	Cha.	A-F	
life factors	Prop.	30°	2.77	2.77	2.96	2.92
		45°	2.75	2.72	2.95	2.96
		90°	2.39	2.38	2.12	2.13
	Non-Prop	135°	2.79	2.77	3.16	3.19
		180°	2.93	2.91	2.98	3
		180°	2.55	2.55	2.28	2.28

models are under life factor of 3, while the values for the non-linear plasticity models are over 3. In contrast, strain energies in the non-linear models have more desirable contributions. In the multi-surface models, however, they often collect around the line of the maximum life factor. Since the plastic strain is dependent on the hysteresis loop shape, various cases in the different loading paths have occurred. All of the prediction ranges are summarized in Table III under different loading paths for a 1% Cr-Mo-V steel.

Overall, fatigue life in the strain energy model is better predicted using the multi-surface plasticity models compared to the other models in different loading conditions. Finally, the Garud model is selected as optimum plasticity model in the proportional and non-proportional loadings for the material (Fig. 3).

Using this approach, the prediction ranges in the presented results are reasonable and analogous according to other methods of plastic strain energy. Garud [12] verified his plastic work model to proportional and non-proportional out-of-phase test data generated for the given metal. For this material, life factor of 3 was predicted by his approach.

6. Conclusions

The cyclic plasticity models of multi-surface and non-linear hardening have been examined by an energy-based criterion under tension-torsion loading in different paths. For this purpose, the fatigue life of a metal was predicted by the plastic strain energy approaches of the plasticity models of Garud, Mroz, Chaboche, and Armstrong-Frederick. A mean fatigue life factor of 3 has been obtained for the models, which is close to the results of other research. The Garud multi-surface model is selected as the optimum plasticity model in the given loading condition.

Nomenclature

a_{ij}	: Tensor of yield surface center or back stress
c, γ	: Material constants from cyclic stress-strain
C, C_s	: Axial and shear fatigue toughness exponents
da_{ij}	: Increment of yield surface center
ds_{ij}	: Increment of stress tensor
$d\varepsilon_{ij}^p$: Strain tensor of the plastic increment
$d\varepsilon_e^p$: Variations of accumulated plastic strain
E_f', W_f'	: Axial and shear fatigue toughness

K_p	: Plastic tangent modulus in multiaxial state
n_{ij}	: Normal vector on the active yield surface
N_A	: Fatigue life in a purely axial loading
N_f	: Predicted fatigue life
N_T	: Fatigue life in a purely torsional loading
R_r	: Stress value at the end of the i th surface
S_{ij}	: Instantaneous deviated stress tensor
ΔW	: Plastic strain energy
ΔW_A^p	: Axial plastic strain energy
ΔW_T^p	: Shear plastic strain energy
σ_{y0}	: Initial yield stress

References

- [1] B. R. You and S. B. Lee, A critical review on multiaxial fatigue assessments of metals. *International Journal of Fatigue*, 18 (4) (1996) 235-244.
- [2] A. Fatemi and D. F. Socie, Critical plane approaches to multiaxial fatigue damage including out-of-phase loading. *Fatigue & Fracture of Engineering Materials & Structures*, 11 (3) (1988) 149-165.
- [3] E. Macha and C. M. Sonsino, Energy criteria of multiaxial fatigue failure. *Fatigue & Fracture of Engineering Materials & Structures*, 22 (1999) 1053-1070.
- [4] I. V. Papadopoulos, P. Davoli, C. Gorla, M. Fillippini and A. Bernasconi, A comparative study of multiaxial high-cycle fatigue criteria for metals. *International Journal of Fatigue*, 19 (3) (1997) 219-235.
- [5] D. H. Kwak, H. R. Roh, J. K. Kim and S. B. Cho, A study on fretting fatigue life prediction for Cr-Mo Steel (SCM420). *Journal of the Korean Society of Precision Engineering*, 24 (4) (2007) 123-130.
- [6] G. Rashed, R. Ghajar and G. Farrahi, Multiaxial stress-strain modeling and effect of additional hardening due to nonproportional loading. *Journal of Mechanical Science and Technology*, 21 (8) (2007) 1153-1161.
- [7] H. J. Gough, Engineering steels under combined cyclic and static stresses. *Journal of Applied Mechanics*, 50 (1950) 113-125.
- [8] Y. Yokobori, H. Yamanouc and S. Yamamoto, Low cycle fatigue of thin-walled hollow cylinder specimens of mild steel in uniaxial tests at constant strain amplitude. *International Journal of Fracture Mechanics*, 1 (1965) 3-13.
- [9] C. E. Feltner and J. Morrow, Microplastic strain hysteresis energy as a criterion for fatigue fracture. *Journal of Basic Engineering, Transactions of the ASME, Series D*, 83 (1961) 15-22.
- [10] J. Morrow, Cyclic plastic strain energy and fatigue of metals. *Internal friction, damping and cyclic plasticity, ASTM STP 378, American Society for Testing and Materials, West Conshohocken, PA*, (1965) 45-87.
- [11] G. R. Halford, The energy required for fatigue. *Journal of materials*, 1 (1) (1996) 3-18.
- [12] H. Jahed and A. Varvani-Farahani, Upper and lower fatigue life limits model using energy-based fatigue properties. *In-*

- ternational Journal of Fatigue*, 28 (2006) 467-473.
- [13] M. Haffman and T. Seeger, A generalized method for estimating multiaxial elastic-plastic notch stresses and strains, part1. *Journal of Engineering Materials and Technology*, 107 (1985) 250-254.
- [14] D. McDowell, An evaluation of recent developments in hardening and flow rules for rate-independent, nonproportional cyclic plasticity. *ASME, Journal of Applied Mechanics*, 54 (1987) 323-334.
- [15] Y. Dafalias and E. Popove, Plastic internal variables formalism of cyclic plasticity. *ASME, Journal of Applied Mechanics*, 43 (1975) 645-651.
- [16] S. Bari and T. Hassan, Kinematic hardening rules in uncoupled modeling for multiaxial ratcheting simulation. *International Journal of Plasticity*, 17 (2001) 885-905.
- [17] W. Prager, A new method of analyzing stresses and strains in work hardening. *Journal of Applied Mechanics*, 23 (1956) 493-496.
- [18] P. J. Armstrong and C. O. Frederick, A mathematical representation of the multiaxial Bauschinger effect. *G.E.G.B. Report RD/B/N731, Berkeley Nuclear Laboratories*, (1966).
- [19] J. L. Chaboche, Time-independent constitutive theories for cyclic plasticity. *International Journal of Plasticity*, 2 (2) (1986) 149-188.
- [20] J. L. Chaboche, Constitutive equations for cyclic plasticity and cyclic viscoplasticity. *International Journal of Plasticity*, 5 (3) (1989) 247-302.
- [21] J. L. Chaboche, On some modifications of kinematic hardening to improve the description of ratchetting effects. *International Journal of Plasticity*, 7 (7) (1991) 661-678.
- [22] Z. Mróz, On the description of anisotropic work-hardening. *Journal of the Mechanics and Physics of Solids*, 15 (1967) 163-175.
- [23] Z. Mróz, An attempt to describe the behavior of metals under cyclic loads using a more general workhardening model. *Acta Mechanica*, 7 (2) (1969) 199-212.
- [24] Y. S. Garud, Multiaxial fatigue: a survey of the state of the art. *Journal of Testing and Evaluation*, 9 (1981) 165-178.
- [25] J. Yanyao, O. W. Christian, V. Michael and N. Horst, Fatigue life predictions by integrating EVICD fatigue damage model and an advanced cyclic plasticity theory. *International Journal of Plasticity*, 25 (5) (2009) 780-801.
- [26] D. Lohr, R. and E. G. Ellison, Biaxial high strain fatigue testing of 1% Cr-Mo-V steel. *Fatigue of Engineering Materials & Structures*, 3 (1980) 19-37.
- [27] K. Kanazawa, K. J. Miller and M. W. Brown, Cyclic deformation of 1% Cr-Mo-V steel under out-of-phase loads. *Fatigue of Engineering Materials & Structures*, 2 (1979) 217-228.
- [28] M. W. Brown, K. J. M., Biaxial cyclic deformation behaviour of steels. *Fatigue of Engineering Materials & Structures*, 1 (1979) 93-106.



Shahram Shahrooi received his B.S. and M.S. degrees in Mechanical Engineering from the Islamic Azad University, Arak branch, Iran, in 1991 and 1996, respectively. At present, he is a Ph.D. student at the Department of Mechanical Engineering at the University of Malaya, Kuala Lumpur, Malaysia. Mr. Shahrooi's research interests include fatigue, plasticity, and finite element method.



Ibrahim Henk Metseelar earned his M.S. degree in Chemical Technology from the University of Twente in the Netherlands in 1994. During his Ph.D. studies in Mechanical Engineering, his research focus was Tribology. Dr. Metseelar joined the University of Malaya in September 2001 and has worked as Senior Lecturer in the Materials program in the Mechanical Engineering Department.